RECENT RESULTS FROM DESY*

By L. Criegee

DESY, Hamburg**

(Received November 2, 1982)

The important field of $\gamma\gamma$ reactions will be covered by Drs. A. Bäcker and H. Kolanoski. For more details about electroweak effects observed at PETRA the reader is referred to the report of Prof. J. Branson. The term "recent" in the title refers essentially to the time span between the Bonn Conference and May 1982.

PACS numbers: 13.60.–r

1. Storage ring news

A survey of the DESY facilities with the e^+e^- storage rings DORIS and PETRA, and the active detectors is shown in Fig. 1. Both DORIS and PETRA have been considerably improved during the past years and will further be improved in the next future. The resulting higher luminosities allowed the investigation of small effects like the interference between the electromagnetic and the weak neutral current. The energy increase of the storage rings may bring significant measurements in the Υ and hopefully also in the toponium range.

* Presented at the Fifth Warsaw Symposium on Elementary Particle Physics, Kazimierz, Poland, May 1982 and at the XXII Cracow School of Theoretical Physics, Zakopane, Poland, May 30 — June 9, 1982.

** Address: DESY, Notkestr. 85, 2000 Hamburg 52, W. Germany.

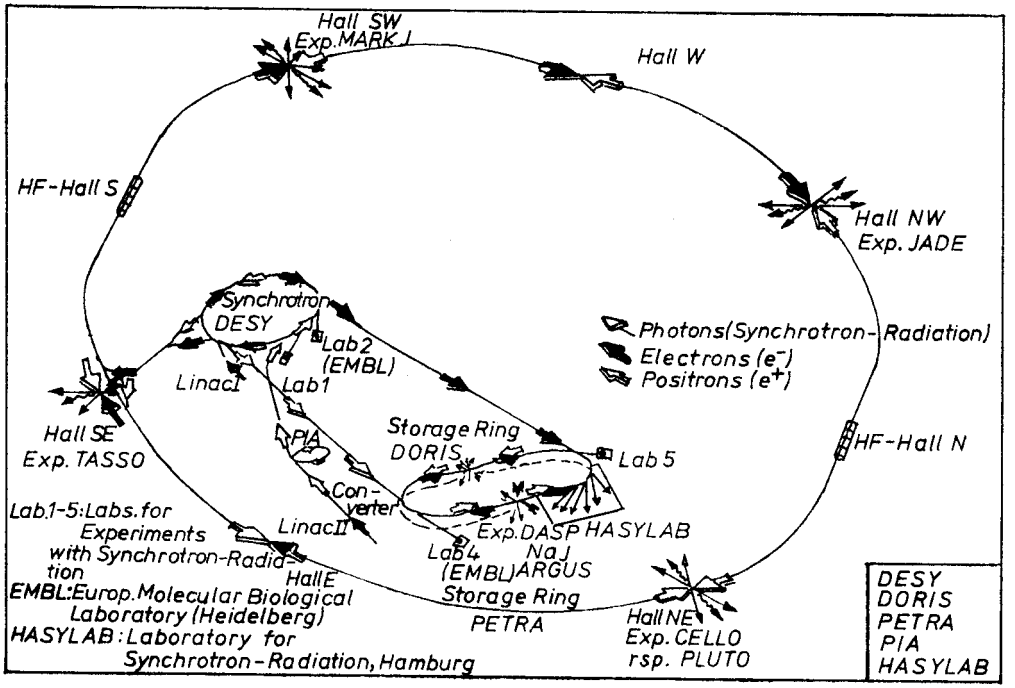

Fig. 1. DESY site with storage rings PETRA and DORIS

1.1. PETRA

The progress in the reachable c.m. energy E_{CM}^{max} and in the luminosity is listed in Table I. The data of 1978 allowed the first look into the new energy regime, with the result that the two-jet character of the events still was consistent with the quark-parton model like at lower energies. The energy and luminosity rise in 1979 then brought the first evidence for a third jet, as resulting from the emission of gluons. No indication for the top meason was found in that, nor in the following year up to 36.6 GeV. A dramatic increase of luminosity was obtained in 1981 through the "mini-beta" focussing in the interaction regions ($\beta_z^* = 8$ cm). This brought, among many other results, the first evi-

TABLE I

PETRA performance

Period	E_{CM}^{max} (GeV)	$\int L dt$ (events/10^{-33} cm^2)
1978 Nov., Dec.	17	40
1979	31.6	4000
1980	36.6	8000
1981	36.6	36000
1982, 1st half	36.6	51000
1982, 2nd half	41	
1983	45	

dence for the $\mu^+\mu^-$ asymmetry originating from the electro-weak interference, as reported on the 1981 Bonn Conference [1, 2] and pursued in section 3 of this report. In summer 1982 the energy will be raised to 41, and during 1983 to 45 GeV. This increase will not only offer a chance to find the top meson, but also bring a dramatic increase in weak neutral current effects, as outlined in Sections 2 and 3.

1.2. DORIS II

During 1978, the storage ring DORIS I, originally designed to cover the c.m. energy range from 1 to 6 GeV, had been upgraded to reach 10.2 GeV. With that machine, the DASP II and PLUTO collaborations produced the first physics results on the Υ resonance. More extensive studies on the Υ and Υ' resonances were performed by the DASP II and LENA collaborations, of which the latter one included a group of the Kraków Institute of Nuclear Physics [3]. The 10.2 GeV could however only be reached with considerable saturation of the magnets, an accordingly complicated operation of the storage ring, and a high power consumption ($\approx$ 10 MW at 10 GeV). It was therefore decided to rebuild the magnets like shown in Fig. 2. By special shims the magnet gap was reduced from 70

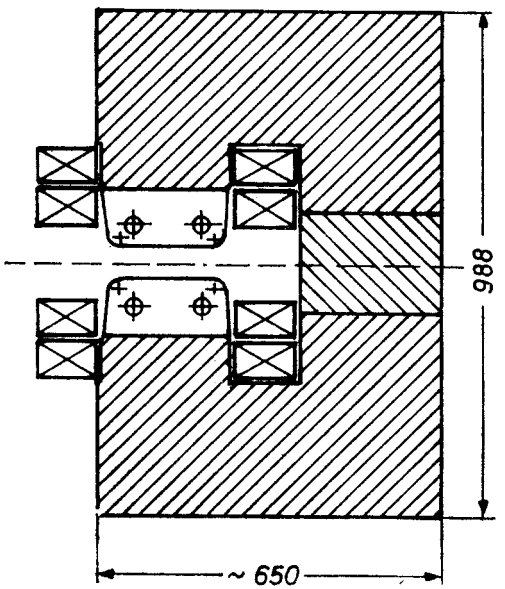

Fig. 2. Cross section of dipole magnet of DORIS II

to 60 mm, thus allowing an operation up to 2×5.6 GeV with little saturation. By also doubling the coil cross section (with the additional coils taken from the obsolete 2nd ring DORIS I) the total power consumption at 10 GeV was reduced to less than 5 MW.

The experience gained in the PETRA construction and operation was used to design the injection path and the optics such as to obtain an "easy to operate" system. Already the first operation brought the rewards of this concept. Table II lists some important dates of the last year.

TABLE II

Start of DORIS II

2 Nov.	1981	end of DORIS I operation
30 Apr.	1982	DORIS II complete
8 May	1982, 12h	first injection
	16h	one revolution
	19h	beam stored
	21h	beam accumulation
12 May		design current reached (25 mA)
23 May		colliding beams $4.8+4.8$ GeV
15 July		peak luminosity 8×10^{30} cm^{-2} sec^{-1}
10 Aug.		Υ resonance located by Crystal Ball, first data

The Crystal Ball collaboration again includes the Institute of Nuclear Physics at Kraków. The neutral energy resolution of this detector should allow, among other things, to resolve the rich spectrum of P-states in the $\Upsilon(1S)$ to $\Upsilon(3S)$ region, which seems not to be possible for the CUSB detector at the Cornell storage ring, and thus provide new insight into the quark-quark potential.

2. $e^+e^- \to$ *hadrons*

Through the quark-parton model (QPM), hadron production in e^+e^- annihilation has been very successfully reduced to the creation and subsequently fragmentation of $q\bar{q}$ pairs (Fig. 3a). The following sections will concentrate on tests of those modifications which are introduced by the weak neutral current (Fig. 3b), and by the emission of gluons as predicted by QCD (Fig. 3c and higher orders).

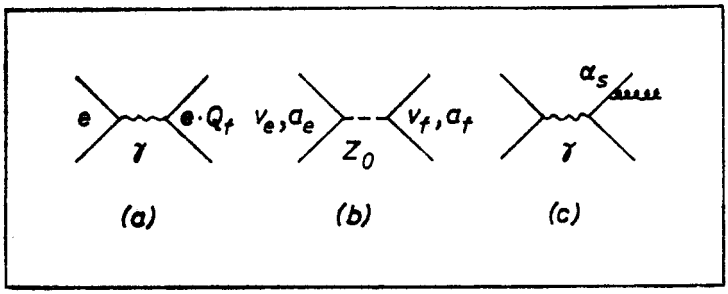

Fig. 3. Diagrams contributing to σ_{tot}

2.1. The total cross section

From the diagrams of Fig. 3 one obtains the total cross section for hadron production in units of the electromagnetic muon pair cross section, called R, as:

$$R \equiv \frac{\sigma_{tot}(e^+e^- \to \text{hadrons})}{\sigma_{QED}(e^+e^- \to \mu^+\mu^-)}$$

$$= 3\{\sum_f Q_f^2[1+\alpha_s/\pi+1.4(\alpha_s/\pi)^2]-2s\,g\,\mathrm{Re}\,(\chi)v_e\sum_f (Q_f v_f)$$

$$+s^2g^2|\chi|^2\,(v_e^2+a_e^2)\sum_f (v_f^2+a_f^2)\}$$

with eQ_f the electric charge of quark "f",

$$\alpha_S(Q^2) = 12\pi/(23 \ln (Q^2/\Lambda^2) + 15.1 \ln (\ln (Q^2/\Lambda^2)))$$

the strong coupling constant at $Q^2 = s$ for 5 flavours with the scale parameter $\Lambda \approx 100$–300 MeV,

$$g = G_F/(8\sqrt{2}\,\pi\alpha) = 4.49 \cdot 10^{-5}\ \mathrm{GeV}^{-2},$$

v_e, a_e, v_f, a_f the vector and axial vector coupling constants of electrons (e) and quarks (f), and

$$\chi = M_z^2/(M_z^2 - s + i\Gamma M_z)$$

the propagator of the Z^0 normalized such that it approaches $+1$ at the low s which are presently accessible.

In the Glashow-Weinberg-Salam model, the weak couplings all depend on only one empirical parameter, $\sin^2 \Theta_w$, like

$$v \equiv 2g_v = \pm 1 - 4Q \cdot \sin^2 \Theta_w$$

$$a \equiv 2g_a = \pm 1$$

with the sign depending on the weak isospin, "+" for u and c quarks, and "−" for d, s, b quarks and for the electron.

One should note that the second order QCD-term $1.4(\alpha_S/\pi)^2$ as given in the $\overline{\mathrm{MS}}$ scheme [4] is very small ($< 4 \times 10^{-3}$ at $s = 1000\ \mathrm{GeV}^2$), and indicates that the expansion in α_S/π is rapidly converging, and the prediction can be regarded as "safe". It should also be noted that with the current value of $\sin^2 \Theta_w \approx 0.23$, v and therefore the electro-weak interference term is very small, and the quadratic weak-weak term dominates the correction.

After subtraction of both the QCD and the weak correction, the cross section should then follow the prediction of the quark parton model, $R = 3\Sigma Q_f$ = constant between flavour thresholds. One can test this prediction and the underlying assumption, that quarks are point-like.

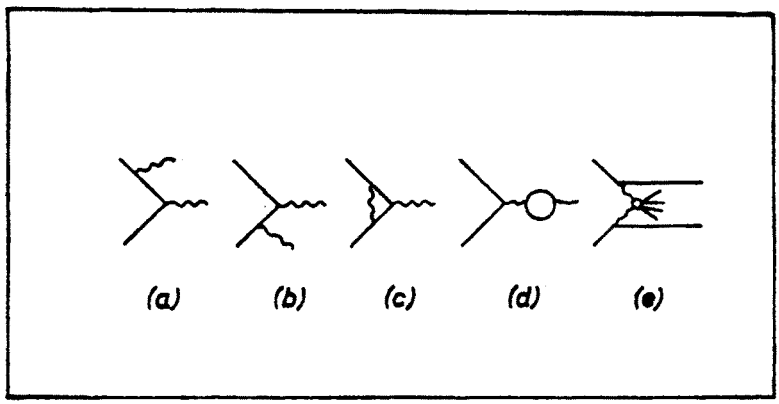

Fig. 4. Radiative corrections (a)–(d) and $\gamma\gamma$ background (e)

A precise measurement of σ_{tot} which would be desirable because of the "hard" prediction available, has to overcome the following difficulties:

1. radiative corrections are rather large (10–30%), because hard photons emitted in the initial state (Figs. 4a, b) lower the energy of the virtual photon such that it sees a higher $q\bar{q}$ cross section. Note that the vacuum polarization given by Fig. 4d has to include the hadronic part as given by the sum over the quark loops ($\sim R$),

2. the acceptance for the jet-like events is to a small extent dependent on the width and other parameters of the parton fragmentation,

3. the luminosity has to be determined from a gauge reaction like Bhabha scattering with its own acceptance and radiation problems,

4. the "$\gamma\gamma$"-process $e^+e^- \to e^+e^-$ + hadrons (Fig. 4e) with the final state e^+ and e^- escaping close to the beam direction, presents a non-negligible background.

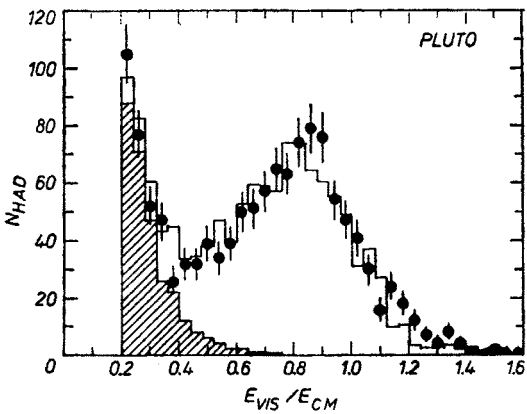

Fig. 5. Number of hadronic events vs E_{vis}/E_{CM}

Fig. 5 shows a measured event distribution over the observed energy, as determined from charged and neutral particles (normalized to the nominal c.m. energy). The data exhibit one broad bump around $E_{vis} = 0.8\,E_{CM}$ which is clearly due to somewhat degraded annihilation events, and a steep rise below $E_{vis} = 0.3\,E_{CM}$. Since beam-gas background has already been subtracted in the plot, this rise originates from e^+e^- collisions, and is attributed to $\gamma\gamma$ reactions (Fig. 4e). A quantitative Monte Carlo calculation based on measurements of the two-photon process [5, 6] indeed shows that $\gamma\gamma$ reactions account for most of the low-energy range, together with a rather long tail from radiative annihilation events (Figs. 4a, b). Since the Monte Carlo program reproduces most of the E_{vis} distribution rather well, the cross section is little dependent on the position of a cut in E_{vis}, if it is applied to both the Monte Carlo generated and the real events. With this cut fixed at $E_{vis} = 0.4\,E_{CM}$, and all corrections applied, the PLUTO collaboration obtained the annihilation cross section R shown in Fig. 6. The cross section agrees with the QCD prediction for 5 flavors (full line from 12–40 GeV), and excludes the production of a sixth quark (uppermost solid line) below 31 GeV. It is on average higher than the prediction

of the quark-parton model (dashed line). If one attributes the excess to the first-order QCD effect (Fig. 3c)[1], one obtains

$$\alpha_S(1000\ \mathrm{GeV}^2) = 0.30 \pm 0.06\ (\mathrm{stat.}) \pm 0.14\ (\mathrm{syst.}) \qquad \text{(PLUTO)}$$

Within the large systematic error (which results from the 4% systematic error of the data), the value of α_S is consistent with the ones resulting from detailed jet studies [7]. It excludes a pure quark-parton description without QCD ($\alpha_S = 0$) by about two standard deviations.

The TASSO collaboration also reports an evaluation of the annihilation cross section with a small (4%) systematic error, based on the detection of charged particles only [8]. As shown in Fig. 7, the measured values of R are also on average larger than expected from the quark-parton model (QPM). The difference may be due to weak and to QCD

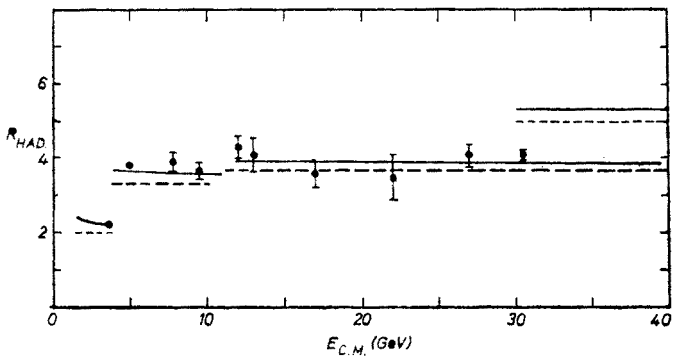

Fig. 6. R vs E_{CM} (PLUTO [6]) with predictions of QPM (dashed) and QCD (full curve). The low energy points were taken at the DORIS storage ring [7]

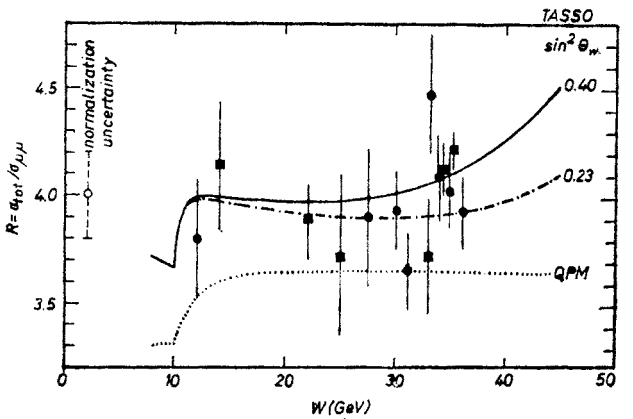

Fig. 7. R vs E_{CM} with predictions of QPM and of electroweak theory (incl. QCD)

[1] Weak effects are negligible below 32 GeV, see below.

effects. Taking the weak effects as known (GWS theory with $\sin^2 \Theta_w = 0.228$), one obtains

$$\alpha_S(1000\ \text{GeV}^2) = 0.24 \pm 0.05\ (\text{stat.}) \pm 0.13\ (\text{syst.}). \qquad \text{(TASSO)}$$

If, on the other hand, $\alpha_S = 0.17$ is fixed as obtained from the evaluation of 3-jet topologies [7] one finds

$$\sin^2 \Theta_w = 0.40 \pm 0.16\ (\text{stat.}) \pm 0.02\ (\text{syst.}). \qquad \text{(TASSO)}$$

A joint evaluation of all PETRA experiments [1] narrows the value down to

$$\sin^2 \Theta_w = 0.24 \pm 0.06\ (\text{stat.}) \pm 0.02\ (\text{syst.}). \qquad \text{(all PETRA)}$$

Although the error of $\sin^2 \Theta_w$ is still larger than in measurements of neutrino and of polarized electron scattering [1], three points should be noticed:

1. The Q^2 of these measurements is much higher than in the scattering experiments, verifying the point-like couplings of the weak interactions.

2. The weak interactions are tested for five instead of only two quark flavours.

3. The predicted effect increases strongly with energy (Fig. 7), so that forthcoming measurements around 44 GeV will already be much more sensitive.

Are quarks point-like? Possible deviations of R from the standard prediction (QPM with QCD and GWS corrections) can be expressed by a quark form factor $G_M(s)$, with $R \sim |G_M(s)|^2$. If G_M is parametrized by cutoff parameters Λ, one arrives at the following limits (95% C.L):

TABLE III

Cutoff parameters in $q\bar{q}$ production

Function	Cutoff	Experiment
$G_M = 1/(1-s/\Lambda^2)$	$\Lambda > 186$ GeV	TASSO
$= 1/(1-s/\Lambda_-^2)^2$	$\Lambda_- > 264$ GeV	TASSO
$= 1 \pm s/(\Lambda_\pm^2 - s)$	$\Lambda_- > 285$ GeV	MARK J
	$\Lambda_+ > 190$ GeV	MARK J

This means that the cutoff parameters describing unknown deviations from the electroweak $q\bar{q}$ production are of the same magnitude (200 GeV) as those for deviations from the electromagnetic production of e^+e^- and $\mu^+\mu^-$ pairs, and of other QED reactions. In other words, quarks appear to be as small as leptons.

2.2. Scaling violations

The quark-parton model predicts scaling, that is an energy-independent value of R, and of the inclusive particle distributions $1/\sigma\ d\sigma/dx$, with $x = 2E/\sqrt{s}$. QCD effects should be visible in corrections which vary with the logarithm of the energy. These scaling violations were rather small in the case of R, as shown above. Larger ones are expected in the inclusive particle spectra.

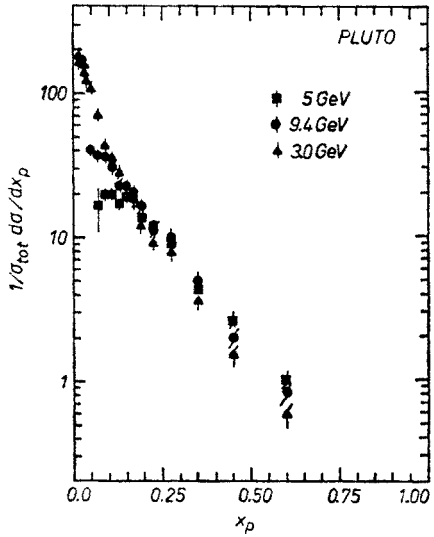

Fig. 8. Inclusive charged hadron spectra vs $x_p = 2p/E_{CM}$

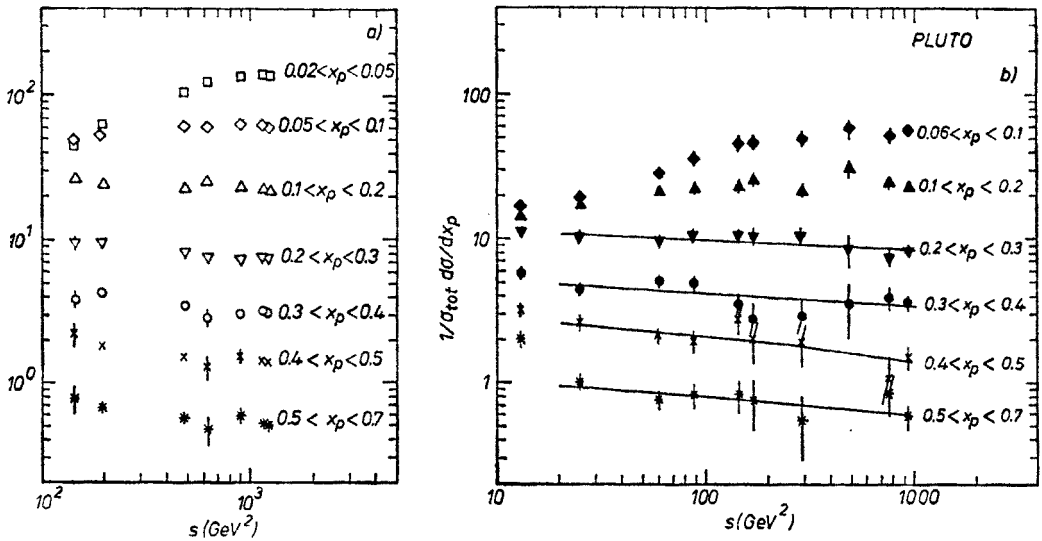

Fig. 9. Energy dependence of inclusive charged hadron spectra. (a) TASSO, (b) PLUTO

Fig. 8 gives the inclusive charged hadron spectra measured at 5.0, 9.4, and 30 GeV. At low x one observes an increase of the spectra with energy, which is trivially attributed to the opening of new flavour thresholds. At $x > 0.3$, the data consistently decrease with the energy, indicating that enhanced gluon emission makes the spectra softer. Figs. 9a and 9b show the same effect plotted as the energy dependence of different x-bins. The high-x cross sections decrease by 20–30%, clearly establishing the scaling violation on

TABLE IV

Fits to scaling violations [9]

x-bin	c (TASSO)	c (PLUTO)
0.1–0.2	-0.033 ± 0.007	
0.2–0.3	-0.071 ± 0.005	-0.051 ± 0.013
0.3–0.4	-0.081 ± 0.006	-0.061 ± 0.017
0.4–0.5	-0.075 ± 0.010	-0.088 ± 0.015
0.5–0.7	-0.074 ± 0.013	-0.074 ± 0.023

a 4–10 σ level. Table IV gives the strength of the scaling violation expressed by the constant c in the parametrisation

$$1/\sigma \, d\sigma/dx = b(1 + c \ln (s/s_0)) \quad (s_0 = 1 \text{ GeV}^2).$$

Both experiments (TASSO and PLUTO) show consistent scaling violations. The quantitative interpretation, however, is unclear at present, since the effect seems to be due to both fragmentation and QCD.

2.3. Inclusive pion spectra

Several PETRA experiments have used their hadron identification facilities to measure particle fractions and specific inclusive hadron spectra. By using two sets of time-of-flight counters, and two different threshold Cerenkov counters (Freon 114 and Aerogel) the TASSO collaboration determined the fraction of pions over the complete range from 0.3 to 10 GeV/c [10].

Fig. 10 gives the fraction of pions as a function of the momentum p. Two points are worth remarking:

(i) The data taken at different c.m. energies, as represented by different symbols, fal

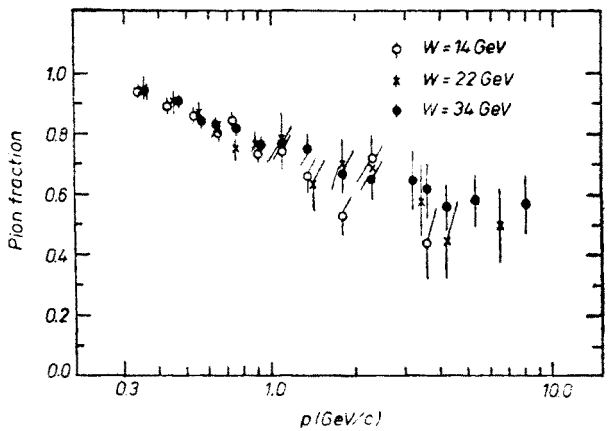

Fig. 10. Pion fraction vs momentum (TASSO)

on top of one another, that is, the pion fraction appears to depend only on p (rather than on $x = 2p/E_{CM}$ alone).

(*ii*) The pion fraction is around 90% at low momenta, but decreases to about 50% at high momenta. The high fraction of non-pions is largely made up by kaons, plus a non--negligible amount of baryons [11].

Fig. 11 compares the scaled pion cross sections $s/\beta\ d\sigma/dx$ taken at 34, 22, 14, and at 5.2 GeV [10, 12]. At medium and high x they decrease slightly with energy, and establish a scaling violation at the 2σ level, if systematic errors are included.

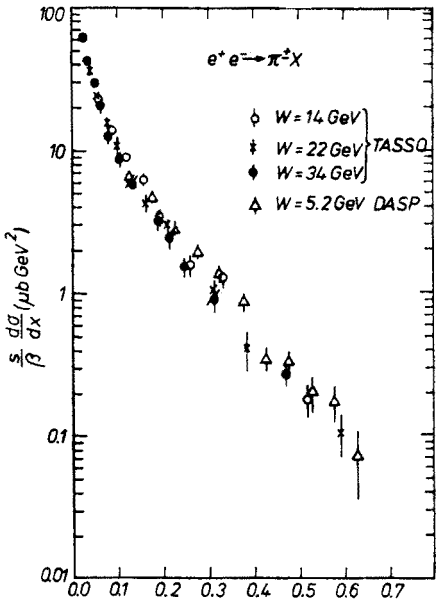

Fig. 11. Inclusive pion cross section vs $x = 2E_\pi/E_{CM}$

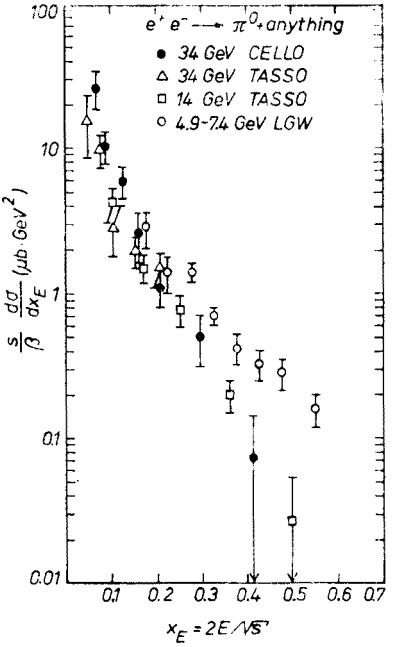

Fig. 12. Inclusive π^0 cross section vs $x = E_\pi/E_{CM}$

The CELLO collaboration has exploited the fine granularity of their liquid argon shower counter to identify neutral pions up to 15 GeV/c [13]. Fig. 12 shows the scaled cross section which was measured at 34 GeV. The comparison with other data taken at 14 GeV [14] and in particular at 5.2 GeV [15] suggests a strong scaling violation. However, it is hard to assess the different systematic errors of the cross sections taken by different detectors. They may in fact simulate a major part of the appearent violation.

2.4. Hard gluon effects.

Way in the past, almost three years ago the first evidence for hard gluons was observed as jet broadening and manifest planar and 3-jet events in e^+e^--annihilation [16]. The strong coupling constant α_S which determines the rate of single gluon emission was found

to be in the range 0.16–0.23. A more precise determination faced at the time two difficulties:
(*i*) fragmentation effects obscure the observation of the hard partons which the predictions of perturbative QCD referred to, and have to be corrected for with the help of empirical models and
(*ii*) unknown or controversial higher order QCD corrections [17] affected the extraction of α_S from the data.

There appears to be a recent convergence considering the importance of the 2nd order correction [18]. The fragmentation process, however, still presents a problem. In the following I want to describe two attempts to minimize the influence of the fragmentation on the analysis:

1. The study of the energy dependence of jet measures. One can state quite generally that fragmentation effects disappear with increasing c.m. energy $\sqrt{s}$ like $1/\sqrt{s}$ or faster, whereas the effects of 1st order QCD that we are interested in depend linearly on α_S and thus only logarithmically on the energy. It should therefore be possible to separate the two contributions, provided one has arguments for believing that they are additive. Given a choice of several jet measures that can be analysed in this fashion, one can try to find those in which the fragmentation part is smallest, or maybe even disappears. One appealing feature of this approach is that it is based on distributions of *all* hadronic events, without any (collaboration-dependent) preselection of "QCD-relevant" topologies.

2. In a completely different approach one classifies the events according to the number of jets they contain, identifies the energies and angles of the jets with those of the QCD partons, and compares the reconstructed parton distributions with those predicted by QCD. As convincing as this method may appear at first sight, the influence of the fragmentation cannot be eliminated completely: Closely spaced partons will produce overlapping jets which cannot be separated, and fluctuations in the fragmentation may produce separated jets out of one hard parton. In order to correct the data for these "spillovers", one has to compute their probabilities using again fragmentation models. One can however try to develop the jet finding algorithms such that the dependence on models and their parameters becomes small.

2.4.1. Energy dependence of jet measures

There is a "classical" prediction [19, 20] of the energy dependence of the mean energy-weighted jet opening angle $\langle E \sin^2 \delta/\sqrt{s}\rangle$, where E is the particle energy and δ the angle with respect to the jet axis. The predicted dependence on $\sqrt{s}$ is

$$\langle E \sin^2 \delta/\sqrt{s}\rangle = 2\alpha_s(s)/\pi + C\langle p_T\rangle/(2\sqrt{s})$$

with $C \approx 3$ from the energy dependence of the multiplicity in the 10–30 GeV energy range ($\langle n_{tot}\rangle = A + C \ln s$), and $\langle p_T\rangle \approx 300$ MeV the mean transverse particle momentum in the jet.

Fig. 13 shows the data [21], corrected for the acceptance and resolution of the PLUTO detector, and their decomposition into the QCD term (dashed line) with its small energy

dependence $\sim 1/\ln s$, and the steeper fragmentation part (difference to full line). The fit gives

$$\alpha_S(1000\ \mathrm{GeV}^2) = 0.18 \pm 0.02,$$

in good agreement with other determinations [16]. Similar results have been obtained from the s-dependence of $\langle 1\text{-}Thrust \rangle$ [21] and of the central plateau height in the energy--energy correlations [22].

As a particularly interesting jet measure the normalized squared jet mass M^2/s has been recently proposed, and in particular the squared mass of the heavy jet $\langle M_H^2/s \rangle$, the light one $\langle M_L^2/s \rangle$, and their difference [23].

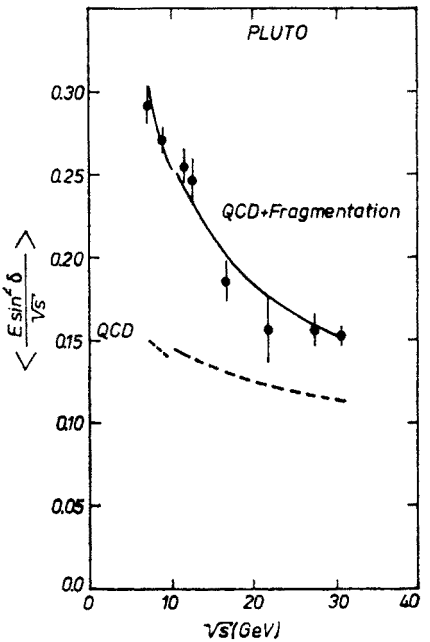

Fig. 13. Weighted jet opening angle vs E_{CM}

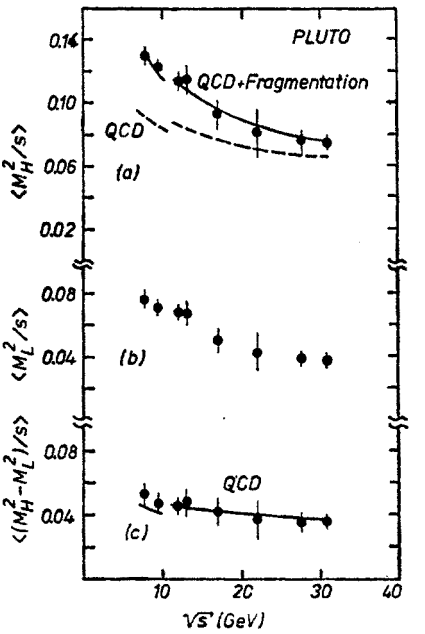

Fig. 14. Squared jet mass vs E_{CM} for (a) the heavy jet, (b) the light one, and (c) the difference

Figs. 14a–c show the apparatus-corrected data in the range $7.7\ \mathrm{GeV} \leqq \sqrt{s} \leqq 31.6\ \mathrm{GeV}$. The fit to $\langle M_H^2/s \rangle$ gives $\alpha_S(1000\ \mathrm{GeV}^2) = 0.20 \pm 0.02$ or 0.15 ± 0.02, depending whether the first or second order expression is used as the QCD prediction [21]. It is evident that the fragmentation part is rather small in $\langle M_H^2/s \rangle$. According to Ref. [23], the fragmentation disappears completely in the prediction for the heavy-light *difference*

$$\langle (M_H^2 - M_L^2)/s \rangle = 1.05(\alpha_S/\pi) + 2.92(\alpha_S/\pi)^2.$$

As shown in Fig. 14c the measured difference shows indeed a very small energy dependence like expected for a pure QCD term. Quantitatively however, a fit gives $\alpha_S(1000\ \mathrm{GeV}^2)$

$= 0.11 \pm 0.02$, not consistent with the values obtained before. The difference perhaps indicates that other effects like higher order QCD corrections, or the heavy-light confusion as produced by fragmentation, cannot be neglected at present energies. Nevertheless the small fragmentation contributions to the average jet masses are remarkable and may be worth pursuing.

2.4.2. Asymmetry of energy–energy correlations

A different observable which was predicted to be free of fragmentation effects and determined only by first-order QCD is the asymmetry of the energy-energy correlation [20]. The correlation function can be defined as a plot of the cosines of all particle-particle angles χ_{ij} of an event, weighted with the product of the two particle energies:

$$f(\cos\chi) = 2\langle \sum_{ij} E_i E_j / s\,\delta(\cos\chi_{ij} - \cos\chi)\rangle.$$

The dominating contribution to the fragmentation was predicted to be symmetric in $\cos\vartheta$, and therefore cancels in the *asymmetry*

$$a(\cos\chi) = f(-\cos\chi) - f(\cos\chi).$$

Fig. 15 shows the asymmetry as measured by the CELLO collaboration [24]. Fragmentation and higher order QCD effects on the energy-energy correlations have recently been investigated in Ref. [25]. The authors find that the fragmentation of the gluon which was neglected above [20] decreases the magnitude of the QCD-predicted asymmetry by about 20%, without affecting the shape in the large-angle range ($|\cos\chi| < 0.7$). The gluon fragmentation therefore just scales up the resulting α_S by 20%. The analysis of Ref. [25] also shows that the 2nd order QCD correction is "well behaved". It changes the predicted

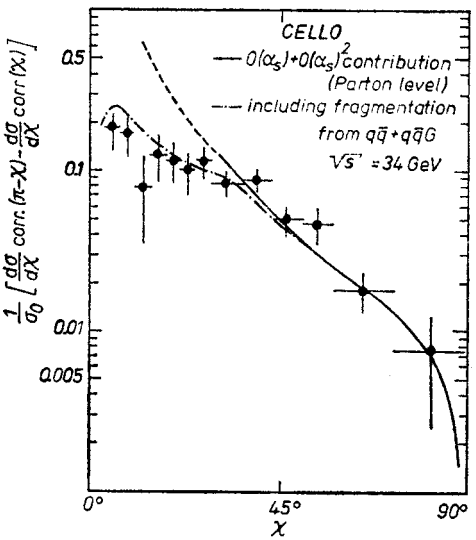

Fig. 15. Asymmetry of energy-energy correlation

asymmetry (at fixed Λ) by only 4%. The full line in Fig. 15 gives the fit of the 1st + 2nd order QCD prediction on the parton level to CELLO data, yielding $\alpha_S(1156\,\mathrm{GeV}^2) = 0.126 \pm 0.01$. The dashed-dotted curve (with the solid continuation) includes the fragmentation effects, and requires a strong coupling constant

$$\alpha_S(1156\,\mathrm{GeV}^2) = 0.148 \pm 0.010,$$

corresponding to

$$\Lambda_{\overline{\mathrm{MS}}} = 278^{+108}_{-90}\ \mathrm{MeV}.$$

The same analysis applied to the PLUTO data [22, 25] gives $\alpha_S(900\,\mathrm{GeV}^2) = 0.142 \pm 0.017$, and

$$\Lambda_{\overline{\mathrm{MS}}} = 168^{+146}_{-103}\ \mathrm{MeV}.$$

It appears that in the energy-energy correlations, especially their asymmetry, both the problems of higher orders of QCD, and of fragmentation, are under control, such as to allow a meaningful determination of the strong coupling constant α_S.[2]

2.4.3. Reconstruction of the parton kinematics

A new jet-finding algorithm has been applied by the JADE group [29]. It uses the invariant two-particle mass M_{ij} as the criterium whether two particles belong to the same jet ($M_{ij}^2 < y^{\max} E_{\mathrm{CM}}^2$, with $y^{\max}$ predefined) or not. If two "belong to the same jet", they are replaced by one pseudo-particle with the added four-momenta. The algorithm starts by replacing the two particles with the smallest invariant mass by such a pseudo-particle, then out of the new set of (pseudo) particles the two with the smallest invariant mass, and so forth, until all squared two-(pseudo-)particle masses are larger than $y^{\max} E_{\mathrm{CM}}^2$. These remaining pseudo-particles are then called jets, and are compared to the hard partons of QCD.

One particular advantage of the algorithm is that the parameter $y^{\max}$ can be easily taken over into the calculation of the QCD cross section. $y^{\max}$ then defines a limit below which two partons should not be separated, but rather treated like one, and below which the cross section has to be calculated in the next lower order [30].

Fig. 16 shows the distribution of the parton thrust x_1 as extracted from the 3-jet class and corrected for contributions other than from 3-parton events. The full curve gives the expectation for the 3-parton topology calculated in 2nd order QCD [17, 30], with the same $y^{\max} = 0.04$ as used for the data. In the range $0.75 \leqq x_1 \leqq 0.85$ the systematic errors from fragmentation and from higher jet multiplicities are particularly small. A fit over this range gives

$$\alpha_S(1000\,\mathrm{GeV}^2) = 0.16 \pm 0.015\,(\mathrm{stat.}) \pm 0.03\,(\mathrm{syst.}).$$

The comparison in this range and therefore the resulting α_S is insensitive to variations of $y^{\max}$, and also to the choice of the fragmentation model. The dashed curve gives the

[2] This conclusion has very recently been challenged by the CELLO collaboration, who found that a description of the fragmentation by the LUND Monte Carlo [26] instead of the one by Hoyer et al. [27] reduces the observable asymmetry drastically, and requires $\alpha_S = 0.25 \pm 0.04$ [28].

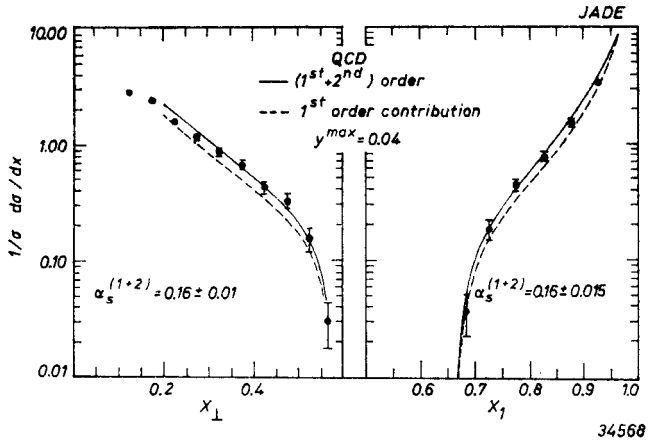

Fig. 16. Distribution of reconstructed parton momenta along (x_1) and perpendicular ($x_\perp$) to the thrust axis

contribution of the first order QCD calculated with the same value of α_S, and demonstrates that the contribution of the second order is not large, and the expansion probably well convergent. (Adjusting the first order prediction alone would lead to $\alpha_S = 0.19 \pm 0.015 \pm 0.03$, not too different.)

It so appears that the QCD prediction is well convergent, and the comparison to the data insensitive to cuts in jet masses, and to the fragmentation model, so that all necessary conditions for a meaningful determination of α_S are fulfilled.

2.4.4. Indications of 4-parton topologies

In second-order QCD the following four-parton final states (plus permutations) are produced

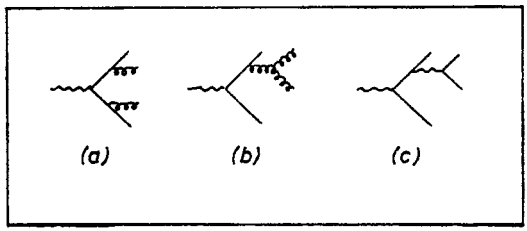

Fig. 17. QCD diagrams yielding four partons

In order to isolate 4-parton from 3- and 2-parton topologies, on can use the observable *acoplanarity*

$$A = 4 \min \left\{ \frac{\sum_i |\vec{p}_i^{\perp}|}{\sum_i |\vec{p}_i|} \right\}^2 ,$$

where $\vec{p}_i$ are the momenta of the partons (or hadrons, see below), and $\vec{p}_i^{\perp}$ their components perpendicular to a plane which is obtained by the above minimizing procedure. Of course, 2- and 3-parton events lie in a plane, and have $A = 0$.

The fraction δ of 4-parton events can then be defined by a cut in A as [31]

$$\delta = \sigma(4 \text{ partons}, A > 0.05)/\sigma_{\text{tot}}.$$

The 4-parton fraction from diagrams 17a, b [3] can be calculated acc. to Ref. [32] (with $\alpha_S = 0.17$) as

$$\delta = 0.05.$$

After fragmentation, the 4 partons will on average produce events with a larger acoplanarity (on the hadron level) than 2 and 3 partons. Fig. 18 shows the distribution of the measured acoplanarity as computed from the hadrons (charged and neutral ones) [31]. It is compared to one model with $\delta = 0.08$, ("L 234", solid histogram), and one with $\delta = 0$ ("L 23",

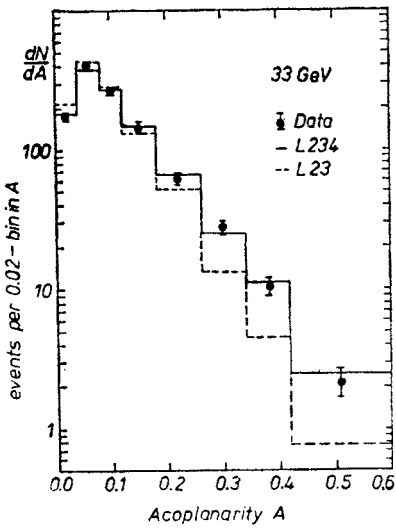

Fig. 18. Acoplanarity distribution

dashed histogram). Clearly, $\delta \simeq 0$ does not fit the data. This is also true if a wider fragmentation function ($\sigma_q = 390$ instead of 350 MeV) is used. Inclusion of the 4-parton events (L 234), on the other hand, fits the data very well, with the best value $\delta = 0.082 \pm 0.012$ at 33 GeV. No effect is observed at 22 GeV, in accordance with QCD expectation. By means of a more involved procedure,[4] the best value obtained by the JADE collaboration is

$$\delta = 0.072 \pm 0.012,$$

consistent with the canonical value of 0.05.

[3] (c) is expected to yield less than 10% in comparison, and is neglected.

[4] In this procedure a 4-jet topology is enforced upon every event, and the four jet momenta are used to calculate thrust T, acoplanarity A, and "tripodity" D_3, a new quantity describing the event symmetry around the thrust axis [33]. The thrust algorithm produces two separate event classes, class I in which the thrust axis is determined by two momentum vectors, and class II in which it coincides with the largest momentum. Class I has $D_3 = 0$, and class II $D_3 = D_3^{\max}(A)$. The four-jet fraction δ is then obtained by simultaneously fitting the A-distribution in class I and the D_3-distribution in class II, and leads to a value consistent with the one obtained with the straightforward procedure.

3. $e^+e^- \to \mu^+\mu^-$

With increasing c.m. energies, effects of the weak neutral current should be observable in the muon pair production. Far away from the Z^0 pole, the cross section can be written as

$$4s/\alpha^2 d\sigma/d\Omega = (1+\cos^2\Theta)(1-2v^2sg+(v^2+a^2)^2s^2g^2)+4\cos\Theta\cdot(-a^2sg+(v^2+a^2)^2s^2g^2)$$

with

$$g = G_F/(8\sqrt{2}\,\pi\alpha) = 4.49\cdot 10^{-5}\ \mathrm{GeV}^2,$$

and v, a the vector and axial vector couplings of the Z^0 to the electron and muon.

In the Glashow-Weinberg-Salam (GWS) theory, one has

$$v \equiv 2g_v = -1+4\sin^2\Theta_w, \qquad a \equiv 2g_a = -1.$$

The cross section has one odd, parity violating term in $\cos\Theta$ which leads to a forward--backward asymmetry of the angular distribution. Integrating $\cos\Theta$ up to $\cos\Theta^{max}$ one obtains the leading contribution to the asymmetry as:

$$A_{\mu\mu}(\Theta^{max}) = -(3/2)a^2\cdot s\cdot g\cdot 4\cdot\cos\Theta^{max}/(3+\cos^2\Theta^{max}).$$

At the time of the 1981 Bonn Conference two of the PETRA experiments could exclude zero asymmetry by more than 2σ, and all the combined ones by 3.2σ [1]. With the high accumulated luminosity of PETRA, the experiments have now collected so many events that three of them independently observe a non-zero asymmetry by more than four standard deviations. Fig. 19 shows the angular distribution from four PETRA experiments as of May 1982 [34]. The backward enhancement and the forward depression as compared to the symmetric QED prediction are clearly visible.

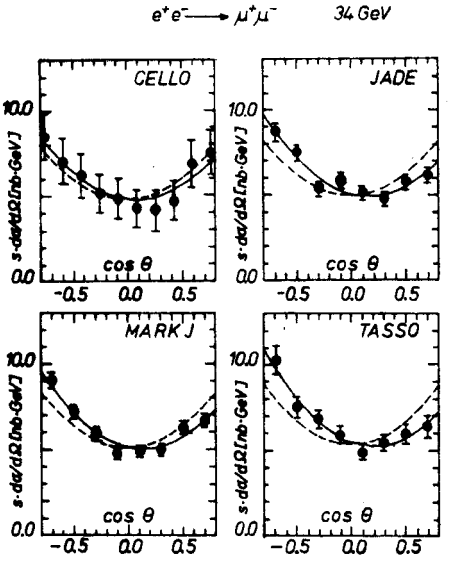

Fig. 19. Angular distribution of muon pairs

TABLE V

Forward-backward asymmetries

$\sqrt{s}$ (GeV)	Experiment	$A_{\mu\mu}(\%)$	$A_{\tau\tau}(\%)$
29	MAC (PEP)	-4.4 ± 2.4	-1.3 ± 2.9
34.2	CELLO (PETRA)	-6.4 ± 6.4	-10.3 ± 5.2
34.6	JADE (PETRA)	$-10.8\pm2.2\pm1$	-7.9 ± 3.9
34.6	MARK J (PETRA)	-10.4 ± 2.1	-7.4 ± 4.6
34.6	TASSO (PETRA)	-10.4 ± 2.1	-5.6 ± 4.4

Table V gives the asymmetries as presented at the Paris Conference [35], which still contain somewhat higher statistics. The values have been extrapolated to $\cos\Theta^{max} = 1$, and corrected for radiative effects in the electromagnetic, but not in the weak amplitude.

The average asymmetry measured in the PETRA experiments is $-(10.4\pm1.3)\%$, in very good agreement with the predicted -9.3% of the GWS theory (with $\sin^2\Theta_w = 0.228$).

The electroweak interference can also be observed, with reduced statistics, in the $\tau^+\tau^-$ production. The PETRA values given in the last column of Table V average to $(-7.9\pm2.3)\%$, also distinctly different from zero, and consistent with the GWS value -9.3%.

Therefore, the electroweak interference as predicted by the GWS theory has to be considered as safely established. Fitting a and v to the combined e^+e^-, $\mu^+\mu^-$, and $\tau^+\tau^-$ cross sections and asymmetries, one finds (assuming lepton universality):

$$a^2 = 0.13\pm0.14, \quad v^2 = -0.06\pm0.13,$$

corresponding to

$$\sin^2\Theta_w = 0.26\pm0.05,$$

in good agreement with the average of the neutrino experiments, $\sin^2\Theta_w = 0.228\pm0.009$ [36]. For models with two neutral bosons [37, 38], Z_1, Z_2, the data also set limits on their spacing from the canonical Z^0 mass. The models lead to an increased vector coupling v, as compared to the "almost zero" of GWS:

$$v^2 \to (-1+4\sin^2\Theta_w)^2 + 16C$$

$$C \sim (1-M_z^2/M_2^2)\cdot(M_z^2/M_1^2-1) > 0.$$

The small v^2 observed at PETRA limits C to

$$C < 0.02 \text{ at } 95\% \text{ C.L.}$$

and thereby sets stringent limits on the deviations of two boson masses from the one of GWS.

In conclusion the PETRA experiments have established a parity violating forward--backward asymmety in muon pair production, in good agreement with the one predicted

from the GWS theory. More detailed tests of electroweak theories, in particular propagator effects which show a finite mass of the Z^0, seem to be in reach once the PETRA energy has been upgraded.

REFERENCES

[1] Proceedings of the 1981 International Symposium on Lepton and Photon Interactions, Bonn 1981, ed. by W. Pfeil, Bonn 1981.
[2] W. Branson, in [1], p. 287.
[3] For latest results see J. K. Bienlein, in [1], p. 190–203.
[4] See W. Celmaster, R. J. Gonsalves, *Phys. Rev.* **D21**, 3312 (1980) and earlier references quoted therein.
[5] PLUTO Collaboration, Ch. Berger et al., *Phys. Lett.* **99B**, 287 (1981).
[6] F. Raupach, thesis, DESY PLUTO-81/05 (1981); W. Lackas, thesis, DESY PLUTO-81/11 (1981).
[7] For reference see L. Criegee, G. Knies, *Phys. Reports* **83**, 152 (1982).
[8] TASSO Collaboration, R. Brandelik et al., *Phys. Lett.* **113B**, 499 (1982).
[9] TASSO Collaboration, R. Brandelik et al., *Phys. Lett.* **114B**, 65 (1982); PLUTO Collaboration, Ch. Berger et al., to be published.
[10] TASSO Collaboration, R. Brandelik et al., *Phys. Lett.* **113B**, 98 (1982).
[11] JADE Collaboration, W. Bartel et al., *Phys. Lett.* **104B**, 325 (1981); TASSO Collaboration, R. Brandelik et al., *Phys. Lett.* **105B**, 75 (1981).
[12] DASP Collaboration, R. Brandelik et al., *Nucl. Phys.* **B143**, 189 (1979).
[13] CELLO Collaboration, H. J. Behrend et al., *Z. Physik* **C14**, 189 (1982).
[14] TASSO Collaboration, R. Brandelik et al., *Phys. Lett.* **108B**, 71 (1982).
[15] D. L. Scharre et al., *Phys. Rev. Lett.* **41**, 1005 (1978).
[16] TASSO Collaboration, R. Brandelik et al., *Phys. Lett.* **86B**, 243 (1979) and earlier presentations quoted therein; *Phys. Lett.* **94B**, 437 (1980); MARK J Collaboration, D. P. Barber et al., *Phys. Rev. Lett.* **43**, 830 (1979); *Phys. Lett.* **89B**, 139 (1980); JADE Collaborati on,W. Bartel et al., *Phys. Lett.* **91B**, 142 (1980) and earlier presentations quoted therein; PLUTO Collaboration, Ch. Berger et. al., *Phys. Lett.* **86B**, 418 (1979); **97B**, 459 (1980).
[17] See R. K. Ellis, D. A. Ross, A. E. Terrano, *Phys. Rev. Lett.* **45**, 1226 (1980); *Nucl. Phys.* **B178**, 421 (1981); K. Fabricius, I. Schmitt, G. Kramer, G. Schierholz, *Phys. Lett.* **97B**, 431 (1980); *Z. Phys.* **C11**, 315 (1982); J. A. M. Vermaeseren, K. J. F. Gaemers, S. J. Oldham, *Nucl. Phys.* **B187**, 301 (1981).
[18] T. Gottschalk, *Phys. Lett.* **109B**, 331 (1982).
[19] A. de Rujula, J. Ellis, E. G. Floratos, M. K. Gaillard, *Nucl. Phys.* **B138**, 387 (1978).
[20] C. L. Basham, L. S. Brown, S. D. Ellis, T. S. Love, *Phys. Rev. Lett.* **41**, 1585 (1978); *Phys. Rev.* **D17**, 2298 (1978).
[21] PLUTO Collaboration, Ch. Berger et al., *Z. Phys.* **C12**, 297 (1982).
[22] PLUTO Collaboration, Ch. Berger et al., *Phys. Lett.* **99B**, 292 (1981).
[23] L. Clavelli, D. Wyler, *Phys. Lett.* **103B**, 383 (1979).
[24] CELLO Collaboration, H. J. Behrend et al., *Z. Phys.* **C14**, 95 (1982).
[25] A. Ali, F. Barreiro, *Phys. Lett.* **118B**, 155(1982).
[26] B. Andersson, G. Gustafson, T. Sjostrand, *Z. Phys.* **66**, 235 (1980); *Nucl. Phys.* **B197**, 45 (1982); T. Sjostrand, Univ. Lund preprint LU TP 80-3 (1980); *Comp. Physics Comm.* **27**, 243 (1982).
[27] P. Hoyer, P. Osland, H. G. Sander, T. F. Walsh, P. M. Zerwas, *Nucl. Phys.* **B161**, 349 (1979).
[28] CELLO Collaboration, H. J. Behrend et al., DESY 82-061 (1982).
[29] JADE Collaboration, W. Bartel et al., *Phys. Lett.* **119B**, 239 (1982).
[30] G. Kramer, DESY 82-029 (1982).
[31] JADE Collaboration, W. Bartel et al., *Phys. Lett.* **115B**, 338 (1982).
[32] A. Ali, J. G. Koerner, Z. Kunszt, J. Willrodt, G. Kramer, G. Schierholz, E. Pietarinen, *Phys. Lett.* **82B**, 285 (1979); *Nucl. Phys.* **B167**, 154 (1980).

[33] O. Nachtmann, A. Reiter, *Z. Phys.* **C14**, 47 (1982).
[34] P. Steffen, Moriond lecture, DESY 82-039 (1982).
[35] M. Davier, *Electroweak and neutral currents*, International Conference on High Energy Physics, Paris, July 1982.
[36] Particle Data Group Compilation, *Rev. Mod. Phys.* **52**, No. 2 (1980), Part II.
[37] E. H. de Groot, D. Schildknecht, G. J. Gounaris, *Phys. Lett.* **90B**, 427 (1980); E. H. de Groot, D. Schildknecht, *Phys. Lett.* **95B**, 128 (1980).
[38] V. Barger, W. J. Keung, E. Ma, *Phys. Rev. Lett.* **44**, 1169 (1980).